1. Introduction

Throughout the whole history of flying, the producers have been always trying to invent better and stronger constructions for their planes. All parts of an airplane have to be strong enough to carry heavy loads and especially the wings. The wings must withstand different loads in all kinds of directions, so the internal structure is key to the success (Collective of Authors, 2016). Not only the construction or sturdiness are important but also the weight of the component.

The shapes and structures of the wings may vary, depending on the use. Airplanes which are aimed to reach long ranges has different internal structures than airplanes designed for search and rescue missions, for instance. The priorities during the design process may differ. Let us apply an example on already mentioned airplanes. During the design process of an airplane for long range flights, the key point is weight, on the other hand, during designing an airplane for search and rescue mission, the stability and speed are important. Each wing construction has its own pros and cons, and their usage depends on the purpose.

There are many industries where the drones can be found: From delivery drones, through search and rescue ones which can be used for laser mapping, to military drones (Bobáľ et al., 2017). Every single drone is unique and built for its own tasks (Fahlstrom and Gleason, 2012). The benefits that drones can offer, are significant. For example, they can carry equipment or devices which are at normal conditions dangerous for airplanes (Turiak et al., 2014).

The presence of drones in air space may can cause worries, but most of those devices are equipped with their own collision avoiding system FLARM (Havel et al., 2017).

2. Current status

Since the beginning of aviation, the designs of an airplanes have changed radically. Not only the outer shapes of an airplanes have changed but also the internal structures, so they can be sturdier and more durable. The full-scale constructions are much more different, while the main difference is obvious in material. The wings on real airplanes may consist of various materials, including wood, types of metal or composite materials such as fiberglass or carbon (Beňo and Bugaj, 2002), whilst the 3D printed wings are made of one material but can be reinforced with the other one. For instance, the wing made of PLA and reinforced with carbon spar.

Use of 3D printed objects, which are supposed to be used in practice, is still not widespread yet. A lot of materials, which can be used in 3D printing are still subjects of observation.

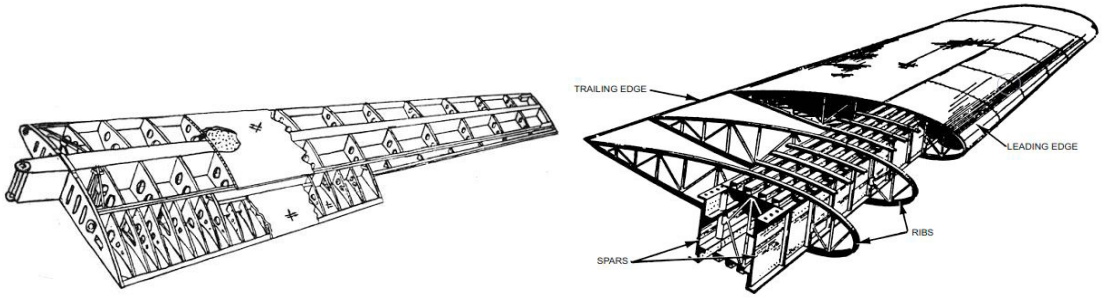

Fig. 1. (left) One spar wing; (right) two spar wing

3. Materials and methods

On the market, there are several methods how to 3D print an object out of various types of materials. The most frequent method is called Fused Deposition Modeling (FDM). Nowadays, the FDM is the most popular and most widespread method to print out 3D objects such as functional prototypes, concept models and manufacturing aids, mostly because of simplicity of the printing. By using this technology, it's possible to achieve really fine details and exceptional strength to weight ratio ("Types of 3D Printers: Complete Guide," n.d.). The printing process consists of

layering melted material layer by layer on the build platform (Fig. 2(left)). This method was also used for printing wings for the purposes of this article.

Another possible printing method is stereolithography (SLA). This printing method is used especially during printing prototypes, mostly because it's accuracy and precision. Stereolithography printing process consists of converting liquid photopolymers into solid 3D objects, layer by layer. Hardening of resin is divided into two phases: In the first phase, the resin is first heated to turn into a semi-liquid form. In the second phase, the resin hardens on contact. Each layer is constructed by using an ultraviolet laser, which is directed by X and Y scanning mirrors ("Stereolithography - Create Concept Models, Cosmetic & Prototypes," n.d.). The whole process of printing runs upside down (Fig. 2(right)).

a. a light-emitting device
b. tank with resin
c. laser selectively illuminates the transparent bottom
d. solidified resin
e. lifting platform.

Once completed, the printed 3D part needs to be cleaned in chemical bath to remove any excess resin.

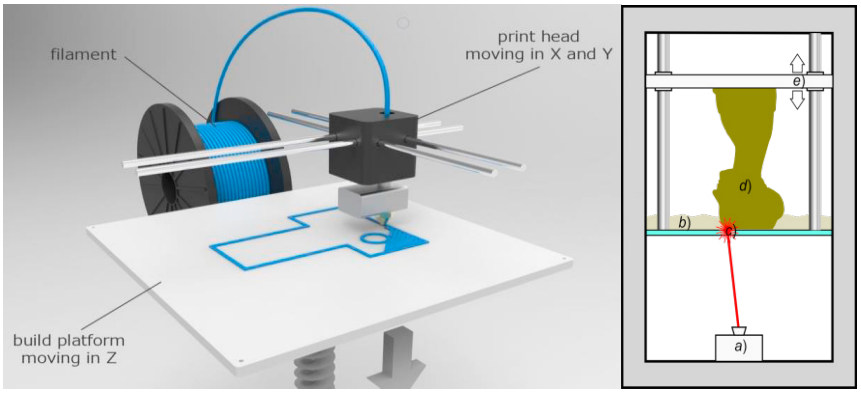

Fig. 2. (left) Fused deposition modeling printing scheme; (right) stereolithography printing scheme

Currently, there are approximately 25 types of filaments on the market. Each of them has its own pros and cons and their usage depends on application. Two most used materials, are PLA (Polylactic Acid) and ABS (Acrylonitrile Butadiene Styrene). Both of these materials are very popular among the users for various reasons.

For this project, the authors have decided to use the most popular out of all filaments, the PLA. There are a few reasons for this decision, such as most accessible filament on the market, good value and performance ratio, easy to work with.

In the beginning of the design process, the suitable airfoil was chosen. In this phase of the project, the airfoil is not that important. The more important is unity of all tested wings. On all wings, NACA2412 airfoil has been used. The main difference can be found inside of the wings. Every single wing has unique internal structure created by using different infill patterns in 3D printing program - Cura.

In 3D printing industry, the following types of infills (Figure 3) are used:

- **Grid:** Strong 2D infill
- **Lines:** Quick 2D infill
- **Triangles:** Strong 2D infill
- **Tri-hexagon:** Strong 2D infill
- **Cubic:** Strong 3D infill
- **Cubic (subdivision):** Strong 3D infill (this saves material compared to Cubic)
- **Octet:** Strong 3D infill
- **Quarter cubic:** Strong 3D infill

- **Concentric:** Flexible 3D infill
- **Concentric 3D :** Flexible 3D infill
- **Zig-zag:** A grid shaped infill, printing continuously in one diagonal direction
- **Cross:** Flexible 3D infill
- **Cross 3D**: Flexible 3D infill:

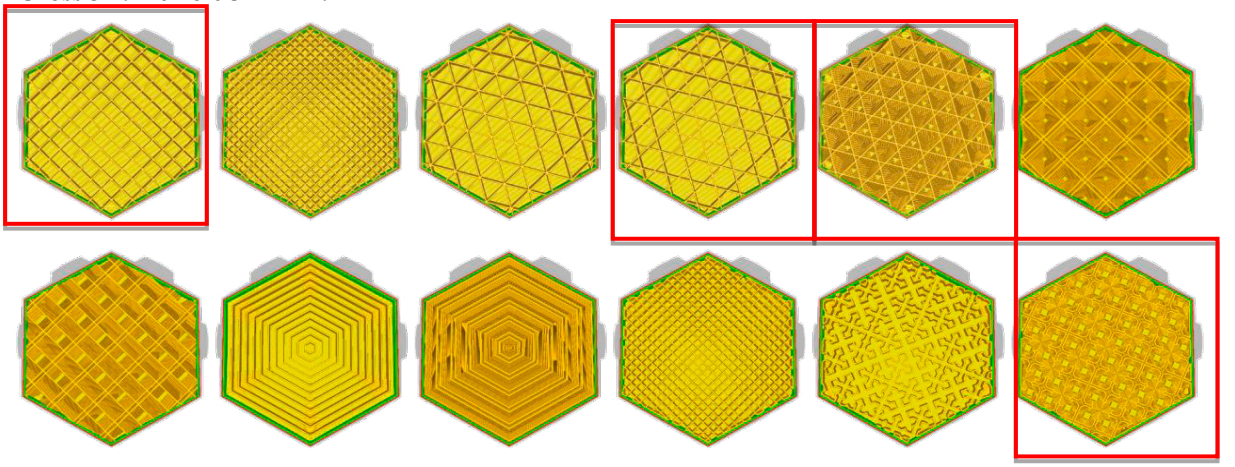

Fig. 3. Basic types of infills used in 3D printed industry ("Ultimaker Cura infill settings," n.d.)

The "Cubic" pattern has been chosen for the less complicated pattern. The "Concentric" pattern showed 0% of the interconnection and in the case of the "Cross" and "Cross-3D" patterns, a better Cross-3D pattern link was clearly visible. Authors selected infiltration types are marked with a red frame. The shape of the "Gyroid" infill is still a relatively new type of pattern, and its image can be found in Fig. 4, where it is visible already in the wings.

The choice of an infill was based on various factors. Since the "triangles" and "tri-hexagons" are not very different in practice, the authors have decided to use the "tri-hexagon" because of the density of an infill. The same applies to "Cubic" and "Quarter-cubic" patterns. The "Cubic" pattern was chosen on the basis of the less complicated pattern, otherwise the decision was made to connect the pattern to the ward cover where the "concentric" pattern displayed 0% of the interconnection, and in the case of the cross "Cross" "And" Cross-3D "was clearly seen to be a larger cross-3D connection. The infiltrated image denotes the selected type of paternity by the red frame. The shape of the gyroid is a relatively new type of pattern and its image is found in Fig. 4 where it is visible right in the wings ("Ultimaker Cura infill settings," n.d.).

All wings were designed for a total weight of 36g along with a support material at the bottom edge. Fig. 4 (left) shows the individual infill directly in the wings. The weight factor affected the total percentage of the infill. The following list shows the percentage of infill for each selected patch: Grid - 10%, Tri-hexagon - 10.5%, Cubic - 10%, Gyroid - 10%, Cross-3D - 9%. All wings samples were printed on the Creality CR-10S printer with the following print settings - material filament: Verbatim - PLA, black, layer height 0,2mm, printing temperature 211°C, build plate temperature: 55°C, shell: 0,4mm wall thickness, 1 perimeter, 3 bottom and top layers, speed: infill and wall speed = 15 $mm \cdot s^{-1}$. The print time of one sample took in average about 10 hours.

Due to the fact that distribution of an infill in the various cross-sections of the wing is at every point different and variable, it is not possible to perform a relevant load simulation of wing samples. For this reason, the samples of the individual infill are verified only by experimental tests and then compared. To verify the properties by simulation, the classic wing structure with lightening holes (Fig. 5) and a known shape in each point of the wing cross section, was selected. The simulation in Ansys 19.2 has allowed to compare the simulated model with the real printed wing and determine the position of the largest bend for the correct positioning of the probe indicator for the experimental measurement. Simultaneously, the simulation has traced the points with the highest concentration of stress and thus allowed the optimization of the construction of the wings for the future research.

Based on these findings, experimental flexure verification was performed with the known load on individual wings. Experimental verification was performed according to the scheme shown in Fig. 6 (left). The wing sample was placed on two supports Fig. 6 (right) at a distance of 175 mm (parameter L) and through the transfer string the sample was pulled by force G. The evaluation parameter was the flexure in the center of the wing L / 2 characterized by the magnitude "y".

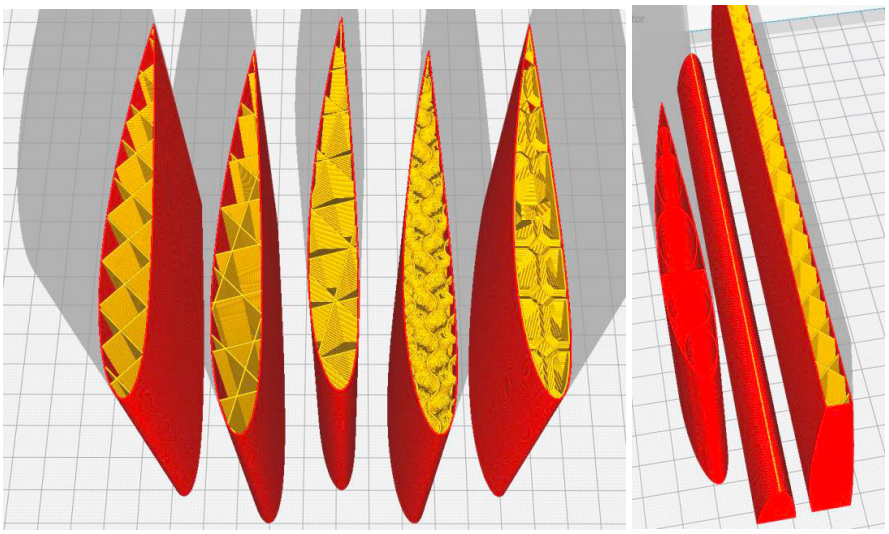

Fig. 4. (left) Demonstration of patterns in sample wings - from the left: Grid, Tri-Hexagon, Cubic, Gyroid, Cross-3D; (right) demonstration of an additional wing with lightening holes and wing with 90° fiber orientation

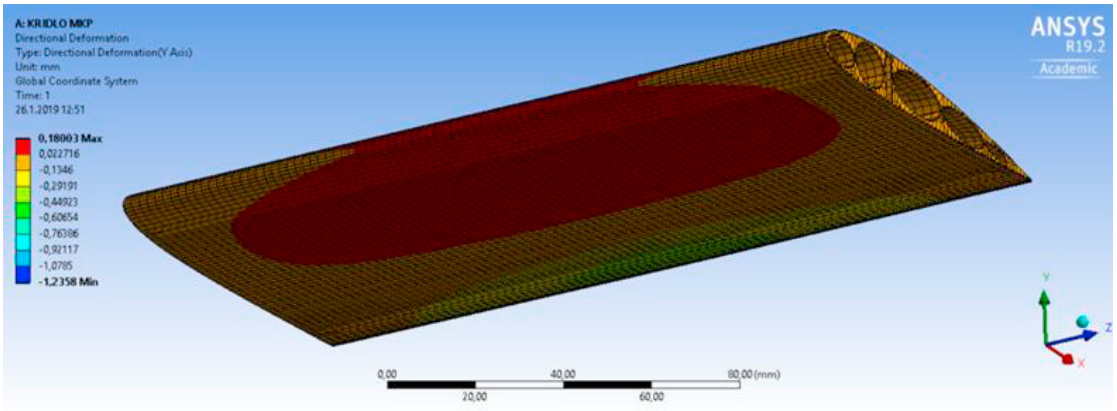

Fig. 5 Simulation of deformation deflections (directional deformation) in “Y” axis

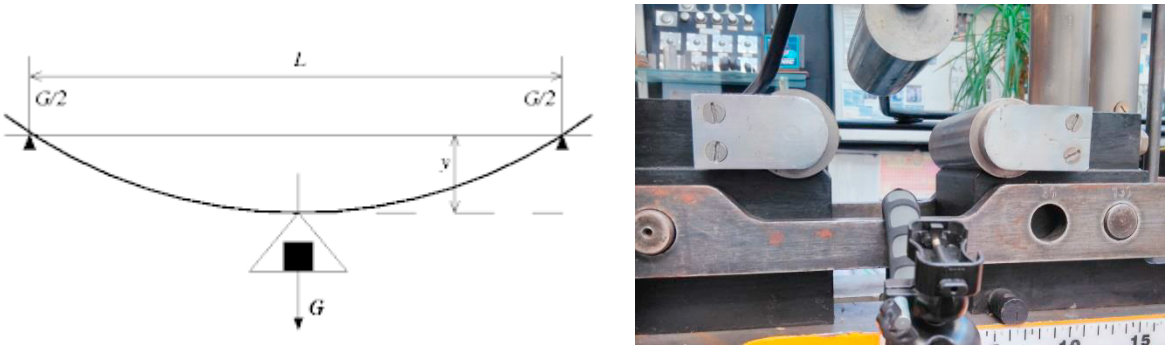

Fig. 6. (left) scheme of experimental flexure verification; (right) image of supports

For a better comparison of not only the various infills and patterns, the authors also printed a sample of the simulated wings (Classic holes wing) that is included in Table 1.

In addition to the shape of the pattern, the direction of the fiber was also taken into account, which is in the case of tested samples due to accurate and effective print, at an angle of 90 degrees to the direction of the stress distribution in the material. For this reason, another wing that has 0 degrees has been printed out.

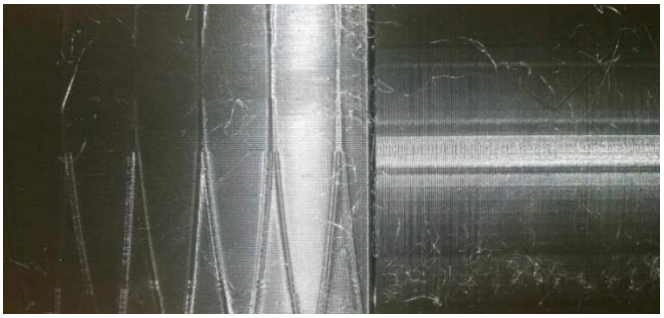

Fig. 7. 90° fiber orientation of “cubic” pattern (left); 0° fiber orientation of “cubic” pattern (right)

4. Results

The parameters and results of quantifiable measurements are shown in Table 1. The graphical representation of the measurement can be seen in Figure 8, which shows the course of the folds with given loads. Sample loading was varied in regular 500-gram steps. The measurements began with a loading of each wing with a reference weight of 100 grams, to ensure the relevancy of the results. Based on the simulation of the known wing with lightening holes, the authors have determined a touch point to measure the deflection at a distance of 60 mm from the trailing edge of the wing.

Based on the definition that elasticity is the ability of an object or material to resume its normal shape after being stretched or compressed without distortion, the individual flexures were compared. From the results, it is possible to define that "Tri-Hexagon" pattern, which is represented in graph by green colour, is the toughest one among the others. The opposite case represents the "Gyrodid" pattern, which exhibits the highest degree of plastic deformation under the same load as the other paterns.

Table 1. Table of measured data

Infill pattern Flexure (mm)	Grid	Tri-Hexagon	Cubic	Gyroid	Cross-3D	Classic Holes	Grid 90°	Force (N)
Measurement 1	0,230	0,160	0,220	0,290	0,200	0,270	0,230	4,905
Measurement 2	0,400	0,340	0,430	0,505	0,425	0,490	0,400	9,81
Measurement 3	0,560	0,505	0,650	0,720	0,640	0,670	0,570	14,715
Measurement 4	0,720	0,675	0,860	0,935	0,870	0,830	0,720	19,62
Measurement 5	0,905	0,840	1,070	1,150	1,075	0,990	0,895	24,525
Measurement 6	1,060	1,000	1,280	1,380	1,290	1,140	1,040	29,43
Measurement 7	1,230	1,160	1,490	1,585	1,480	1,290	1,220	34,335
Measurement 8	1,370	1,320	1,670	1,770	1,690	1,440	1,370	39,24
Measurement 9	1,530	1,440	1,860	1,960	1,875	1,580	1,505	44,145

The opposite case is the "Gyroid" pattern, which exhibits the highest degree of plastic deformation under the same load compared to the other patterns.

An interesting feature is the comparison of the pattern “Grid” and the “Grid 90°”, whose chart progresses are almost identical without significant deviations. As a result of this, it could be assumed that the direction of printing and its effect on the elasticity and stiffness of the wing is negligible but, assuming the force is applied until the failure of the wing, it is highly probable that the "Grid 90°" will be significantly more resilient to the failure despite the same chart progress. This fact results from the technique of printing and thus the method of laying the individual layers, whose contact surfaces create the notches and thus the crack initiation sites.

By including the fact that the most of the wings also have spars in the use of 3D-printed UAVs, the shape and density of an infill serve in particular to increase the stiffness of the wing structure, while the primary bending load transmits the built-in spar. The results showed that the most suitable pattern for printed wings is the "tri-hexagon" pattern. At the same time, experiments have shown that for applications requiring a high degree of elasticity, it is possible to use the patterns as "Cross-3D" or "Gyroid".

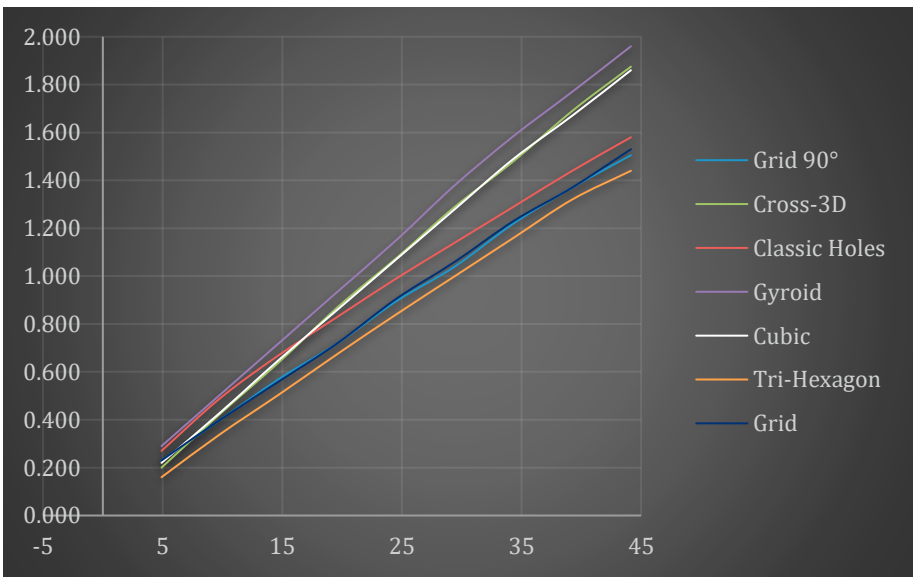

Figure 8. Chart progresses of individual wing samples

Conclusion

The article highlights the strength of the structural units printed on the 3D printer considering their overall strength towards weight and resistance to plastic deformation. By optimal weight / strength ratio, it is possible to increase the overall performance of the printed parts and, in the case of this article, the wing for unmanned flying means. During the study, the authors tried to take into account the factors of the shape of the wing panels, which are non-spar construction. Due to the absence of parameters such as the cross-sectional modulus of elasticity or the overall inhomogeneity of the print, the samples of the wing were verified only by the experimental measurement and they were comparatively compared.

The results of the measurements show that the "Tri-Hexagon" pattern has a most durable design and the "Gyroid" pattern, on the other hand the most flexible. Based on this knowledge, it is possible to integrate and use the individual patterns in practice that requires the given pattern parameters.

The article provides basic data but also serves as a stepping-stone for further research of strength optimization of 3D printed parts, and comparing other criteria such as total stress during deformation or defining flexural modulus. For the sophistication of 3D printing, it is possible, in addition to shape changes, to change the print parameter to open a number of variable factors whose optimization allows the creation of high-strength components. The ratio of the strength and weight of the current 3D prints leads to the competitiveness of 3D industry against composite materials and, in some cases, light metal alloys.

Acknowledgements

The article was created with the support of the science and research development of the foundation “Nadácia Tatra banky”, Faculty of Mechanical engineering, Faculty of Civil Engineering and Air Transport Department at University of Zilina. This paper is an output of the project KEGA No. 011ŽU-4/2018 "New technologies and best practices in education in the Air Transport and Professional Pilots"

Reference

Beňo, L., Bugaj, M., 2002. Materiály v letectví, 1. ed. EDIS.

Bobáľ, P., Sipina, S., Škultéty, F., 2017. Aspects of Aerial Laser Scanning when exploring unknown archaeological sites (Case study). Transp. Res. Procedia 28, 37–44.

Fahlstrom, P.G., Gleason, T.J., 2012. Introduction to UAV systems, 4th ed. ed, Aerospace series. John Wiley & Sons, Chichester, West Sussex.

Havel, K., Balint, V., Novak, A., 2017. A Number of Conflicts at Route Intersections - Rectangular Model. Commun. - Sci. Lett. Univ. Zilina 19.

Stereolithography - Create Concept Models, Cosmetic & Prototypes [WWW Document], n.d. URL https://www.protolabs.co.uk/services/3d-printing/stereolithography/ (accessed 1.31.19).

Turiak, M., Novák-Sedláčková, A., Novák, A., 2014. Portable Electronic Devices on Board of Airplanes and Their Safety Impact. In: Mikulski, J. (Ed.), Telematics - Support for Transport. Springer Berlin Heidelberg, pp. 29–37.

Types of 3D Printers: Complete Guide [WWW Document], n.d. URL https://3dinsider.com/3d-printer-types/ (accessed 1.31.19).

Collective of Authors, 2016. Učebnice pilota 2016: pro žáky a piloty všech druhů letounů a sportovních létajících zařízení, provozujících létání jako svou zájmovou činnost.

Ultimaker Cura infill settings [WWW Document], n.d. URL https://ultimaker.com/en/resources/52670-infill (accessed 1.31.19).